Indian Journal of Biochemistry & Biophysics
Vol. 60, August 2023, pp. 611-623
DOI: 10.56042/ijbb.v60i8.4295

In vitro larvicidal, antioxidant, and DNA binding activity of biosynthesized zinc oxide nanoparticles conjugated with *Andrographis paniculata* aqueous extract

Manish Kumar Dwivedi[1,3] and Prashant Kumar Singh[1,2]*

[1]Department of Biotechnology, Indira Gandhi National Tribal University, Amarkantak-484 887, Madhya Pradesh, India

[2]Department of Biochemistry, University of Lucknow, Lucknow-226 007, Uttar Pradesh, India

[3]Hikal Limited, International Biotech Park, Hinjewadi, Pune-411 057, Maharashtra, India

Received 28 February 2023; *revised 19 July 2023*

Anopheles culicifacies is the major vector responsible for the transmission of human malarial parasite *Plasmodium* sp. The use of green synthesized nanoparticles has emerged as an interesting advancement for the development of plant-mediated insecticides that can be effective against widespread insecticide resistance. In the current study, we report on the larvicidal, antioxidant, H_2O_2 sensitivity, and hemolytic properties of green synthesized zinc oxide nanoparticles using *Andrographis paniculata* (ZnO-APNPs). The ZnO-APNPs were characterized using UV-Visible spectroscopy, FTIR, XRD, and TEM analysis. Crystalline and spherical NPs with an average particle size found to be ~17 nm were synthesized. The UV absorption spectra of the CT-DNA interaction with ZnO-APNPs revealed a bathochromic effect indicating groove binding. The ZnO-APNPs displayed lethality against *A. culicifacies* larvae after 24 h and 48 h of exposure. The LC_{50} and LC_{90}values were 31.75±2.23 ppm and 189.56±2.44 ppm and 95.45±1.56 ppm, 432.36±1.34 ppm at different concentrations respectively. ZnO-APNPs offered complete larval mortality within 24 h and 48 h of exposure. Strong concentration-dependent antioxidant property with a free radical inhibition of 39.51±1.25 % was observed while the ZnO-APNPs were found to be non toxic in hemolysis assay. The strong potency of ZnO-APNPs in killing *A. culicifacies* larvae advocates their further development as potential natural, reliable and ecofriendly larvicides.

Keywords: *Anopheles culicifacies*, *Andrographis paniculata,* Antioxidant activity, Larvicidal, Nanoparticles

Malaria caused by the plasmodium species is transmitted through the bite of infected Anopheles mosquitoes. Mosquitoes belonging to the phylum Arthropoda have been divided into about 3500 species and are distributed worldwide. They are essential factors for various vector-borne diseases[1,2]. They are a necessary target of disease eradication programs as vectors as they transmit infectious agents, causing millions of yearly deaths worldwide[1-5]. The significant genera Culex, Anopheles, and Aedes, are responsible for many fatal diseases such as malaria, yellow fever, dengue, zika, chikungunya, western equine encephalitis, dog heartworm, Japanese encephalitis, *etc*[6]. According to the World Malaria Report (2020), 229 million cases and 409000 deaths were reported due to malaria in 2019. Globally, malaria affected children below the age of 5 years, accounting for 67% (274000) in 2019 (WHO, 2021)[7]. Due to emerging drug resistance and the absence of effective vaccines, the vector control program seems to be an effective technique to control malaria infection or other vector-related diseases. Currently, mosquito larvae are controlled through treatments with organophosphates (temephos, methoprene), insect growth regulators, and bacterial insecticides showing adverse effects on the environment, aquatic organisms, and human health. The persistent and indiscriminate use of synthetic chemical larvicides has led to reduced efficacy[8]. New and effective larvicides that are easily available, cost-effective, biodegradable, eco-friendly, and without any adverse effects on non-target organisms are urgently required.

Medicinal plant extracts have been used as a traditional medicine to treat a wide variety of diseases and disorders such as liver disorders, bowel complaints of children, colic pain, common cold[9], upper respiratory tract infection, fevers, rheumatism, diabetes, arthritis, herpes, dysentery, hepatitis, skin infection, peptic ulcer, snake bites, hypertension, antipyretic, analgesic, protozocidal, antioxidant, anti-HIV, immunostimulant, antimicrobial, anticancer[10], insect sting treatment, influenza, and dyspepsia,

*Correspondence
Phone: + 91-9179122557 (Mob)
E-mail: prashantcdri@gmail.com

dysentery[11]. Phytochemicals present in plants act as great reducing and stabilizing agents during nanoparticle synthesis. The green synthesized nanoparticles have been utilized in diverse bioassays and drug synthesis. They are biocompatible and have increased bioavailability thus reducing the dosage and toxicity associated with synthetic insecticides. Plant-synthesized nanoparticles are more stable compared to those produced by other organisms or other chemical synthesis methods[12].

Large-scale efforts-based botanicals that contain a diversity of phytochemicals have been reported by several workers as larvicidal agents[13]. These phytochemicals act in a synergistic manner and target different biological processes of the mosquito larvae. For enhancing the larvicidal properties of these plant-based insecticides, green synthesized nanoparticles have been developed that carry the insecticidal property of the phytochemicals along with enhanced efficacy. The increased efficiency is attributed to the large surface area to volume ratio of the nanoparticles. These nanoparticles are effective at very low concentrations and can readily penetrate the cell membrane of mosquito larvae[14].

Zinc oxide nanoparticles have received much attention compared to other metal oxide nanoparticles in the recent past. ZnO nanostructures are at the forefront of research due to their unique properties and wide applications[15]. Zinc oxide is an important semiconductor with wide bandgap energy of 3.3eV, and high excitation energy of 60eV making it suitable in bio-molecular detection and diagnostics.

Andrographis paniculata is one of the important tropical traditionally used medicinal plants belonging to the family *Acanthacea* and is usually well-known as the 'King of Bitter' and 'Kalmegh'[16]. It is native to Taiwan, China, India, Hong Kong, Philippines, Malaysia, Indonesia, and many South Asian countries[10]. *A. paniculata* was included in the WHO monograph of 2002 which endorses its medicinal importance[17]. The plant extracts frequently contain complex mixtures of structurally diverse small molecules generally referred to as natural products, secondary metabolites, or phytochemicals. Several natural products from *A. paniculata* have been reported that include furonoidditerpene, 2, 5-dihydroxy-7, 8-dimethoxyflavone-2-o-β-(D)-Glucoside, stigmasta-9 (11), 22 (23)-diene, diterpene glucoside (18), neoandrographolide, flavones-5-hydroxy-7, 8, 2, 3 tetramethoxyflavone, andrographin, 5-hydroxy-7, 8-flavanone, apigenin, 7, 4-dioxymethylether, mono-oxymethylwigthin, deoxyandro-grapholide-19 β-D-glucoside, bitter andrographolide, glucosides, flavonoids, panaculoside, andrographonin, neoandrographolide, and apigenin 7-4-dimethyl etheras major compounds[18]. To date, as per our knowledge, there are no reports on the insecticidal activity using *A. paniculata*-mediated green synthesized zinc oxide nanoparticles. In the current manuscript, we report on the synthesis and characterization of zinc oxide nanoparticles using aqueous leaves extract of *A. paniculata* and its larvicidal properties. The free radicle scavenging activity, H_2O_2 activity, DNA binding studies along with toxicity analysis were performed and reported.

Material and Methods

Chemicals and materials

Analytical grade zinc acetate dehydrates, DMSO, and Sodium hydroxide were purchased from Central Drug House (CDH P Ltd.). Milli-Q Ultra-pure water was obtained from a water purification system (Millipore, Milford, MA, USA). All other reagents used were of analytical grade.

Collection, Authentication, and Extraction process

The whole plant of *A. paniculata* was collected between June and December from the Amarkantak region of Madhya Pradesh (MP), India, and was identified by the Department of Botany, IGNTU, Amarkantak, MP, India. A voucher specimen of the plant (AM/DOB/10) respectively has been deposited for future reference. The collected whole plant was dried and ground to a fine powder. 5 g of powder was measured, added to100 mL of Milli Q water, and boiled at 80°C for an hour. After cooling at room temperature (RT) the mixture was filtered using Whatman filter paper (grade 1) and stored at 4°C till further use.

Biosynthesis of ZnO nanoparticles

The biosynthesis of zinc oxide nanoparticles (ZnO NPs) was undertaken following previously reported methods[19,20]. An equal ratio of filtered extract and 0.02M zinc acetate dihydrate was mixed by keeping the mixture on a hot plate at 60°C with constant stirring at 120 rpm for 2 h. The reaction mixture was divided into three separate tubes and the pH of the mixture was adjusted to 9, 12, and 14 with the addition of NaOH (2N). The mixture was centrifuged at 8000 rpm for 15 min, the supernatant was discarded and the pellet was collected. The pellet was washed

thrice using ethanol and distilled water separately. The wet pellet was kept in a hot air oven at 60°C for drying overnight. This procedure was repeated three times at different temperature conditions (40°C–60°C) for optimization of best synthesis conditions.

Biophysical Characterizations

UV-Visible spectroscopy was used for the analysis of Zinc ions reduction after the addition of 2N NaOH. The UV spectrum scans were recorded at regular intervals at 2, 4, and 6 h after adjusting the pH, with help of a UV-Vis-Spectrophotometer (Shimadzu, UV-1800). The absorption spectrum was re-plotted using UV Probe ver. 2.50 scan from 400-800 nm range. The FTIR spectrum of *A. paniculata* extract and ZnO-APNOs was recorded using an FTIR spectrophotometer (Thermo scientific iD7 Attenuated Total Reflectance-ATR) in the range 4000-400 cm^{-1} to comparatively study the functional groups of phytochemicals present in both the samples. The potential functional groups involved in zinc ion reduction and for capping of reduced ZnO-APNPs were identified and reported. Dried ZnO-APNPs were used for FTIR analysis and the spectrum was recorded in transmittance mode at a resolution of 4 cm^{-1}. The spectrum peaks were obtained and plotted as transmittance at Y-axis and wave number (cm^{-1}) at X-axis.

XRD studies were undertaken to detect the formation and quality of ZnO-APNPs nanoparticles. XRD was performed at parameters 2θ range of 20° to 100° with a divergence slit of 10 mm in 2θ at continuous mode using the D8 Advance XRD system at 1.5406A° wavelength. Estimation of particle size was performed using Scherrer's formula ($D=K\lambda/\beta \cos\theta$).

The morphological analysis of the ZnO-APNPs was performed using transmission electron microscopy (TEM). The microscopic image across the phase transition was probed. The suspended NPs were coated on the copper grid that was allowed to dry under a mercury lamp before imaging. TEM was performed using a dual-tilt liquid-nitrogen-based low-temperature holder (GATAN-636MA) operated in Tecnai G2-20 TEM at 200 kV and 3 mM grid size. For the measurement of CP-ZnO nanoparticles, a magnification of 20,00,000X with ultra-high-resolution 0.2 nm was used.

The zeta potential was measured using Litesizer™ 500 (Anton Paar, Graz, Austria) and analyzed with 1.5 Henry factor and 658 nm laser wavelength. The green synthesized ZnO-APNPs (5 mg) were added to 5 mL of an aqueous solution. Before analysis ZnO-APNPs solution was vortexed for a few min followed by sonication for 5 min.

Biological activities

***Anopheles culicifacies* larval rearing**

The *A. culicifacies* larvae were collected from Pushparajgarh block, Anuppur district, Madhya Pradesh (M.P.), India, and were identified by the Department of Biotechnology, IGNTU, Amarkantak, M.P., India. *A. culicifacies* larvae were maintained in the insectarium at 25-28°C and 60-80% humidity and were fed daily with 5 G of ground dog biscuits and hydrolyzed yeast (Sigma-Aldrich) in a 3:1 ratio[21]. Healthy larvae were collected and used for further bioassays.

Larvicidal activity

The larvicidal activity was performed as per the procedure of the World Health Organization (WHO, 2005). For the bioassay, 10 healthy larvae were transferred to different beakers containing synthesized ZnO-APNPs at different concentrations (10, 50, 100, 200, 300, and 500 ppm) in DMSO along with controls (DMSO and zinc acetate dehydrate at different concentrations). Temiphose was used as standard. Each test was performed three times on different days. The larval mortality was recorded after 24 h and 48 h post-treatment. Prohibiting analysis was used to determine the mortality percentage of larvae along with a median lethal concentration (LC_{50}) and lethal concentration (LC_{90})[22].

***In vitro* hemolysis assay**

Fresh human blood collected in EDTA vial was washed thrice with isotonic Phosphate buffer saline (PBS), pH 7.0 at 25°C by centrifugation (2500 rpm for 10 min). After removing the supernatant, 10% RBC suspension was prepared in PBS from the remaining suspension. Different aliquots (500 µL) of 10% RBC suspension were taken and ZnO-APNPs were added at different concentrations (25, 50, 100, 200 µg/mL) to the individual tubes that were incubated at 37°C for 45 min. The tubes were centrifuged at 2500 rpm for 15 min. Similarly, for maximum hemolysis (positive control) 500 µL of 0.2% Triton-100 was added to the positive control tube while 500 µL PBS was added to the blank tube. After removing the supernatant, the liberated hemoglobin was measured at 540 nm with help of a microplate spectrophotometer (Multiskan sky, Thermo Scientific). The experiment was performed in triplicate and mean ± S.E. was calculated.

$$\% \, Hemolysis = \frac{At-An}{Ac-An} \times 100$$

Where,

At: Absorbance of test sample

An: Absorbance of the control (PBS)

Ac: Absorbance of the control (Triton)

The antioxidant activity of ZnO-APNPs was measured by radical scavenging activity in 2, 2-azinobis (3-ethyl benzthiazoline-6-sulfonic acid (ABTS) assay. The stock was prepared through the mixing of 2:1 (*v*/v) of ABTS (7 mM) and potassium persulphate (2.4 mM) in an aqueous solution. The solution was kept in dark at RT for 16h. Samples were prepared at various concentrations (10, 20, 30, 50, 80, and 100 mg/mL), 1 mL of diluted ABTS solution was added to each tube and incubated at 37°C for 1 h. The measurement was recorded at 734 nm using a spectrophotometer (Shimadzu, UV-1800). For blank and standard reactions DMSO and ascorbic acid were used instead of samples. The percentage inhibition was calculated by using the following formula[23].

Percentage Inhibition (%) = [(Ac − As)/Ac] × 100

H_2O_2 activity

Stock (1 mg/mL) of ZnO-APNPs was prepared in DMSO and to 100 µL solution from this stock, 1 mL of 20 mM H_2O_2 was added and mixed by shaking. The final volume of the reaction was made up to 5 mL using DMSO. The UV spectrum was recorded between 200-800 nm at a regular interval of 15 min.

DNA Binding assay

The DNA binding properties of the ZnO-APNPs was undertaken using UV-Visible spectroscopy (Shimadzu UV–Visible spectrophotometer; UV-1800). CT-DNA (100 µM) salt stock solution prepared in Tris-EDTA buffer (pH-7.4) and kept overnight in the refrigerator. After then we performed UV-Visible spectroscopy for the desired concentrations of CT-DNA at 260 and 280 and found (A260/A280) > 1.8 (1.40), which is indicative that the CT-DNA solution is sufficiently free of protein. The solution of the CT-DNA was stored at 4°C for further experiments. The DNA binding study was performed according to Singh *et al*., (2019)[24]. DNA binding studies between CT-DNA and ZnO-APNPs were done by measuring and analyzing UV–Visible spectra. The spectroscopic changes in absorbance were recorded by keeping constant DNA concentration (100 µM) and varying the concentration of ZnO-APNPs (1 mM, 1.5 mM, 2 mM, 2.5 mM, and 3 mM) in the wavelength range of 220–320 nm.

Statistical Analysis

The LC_{50}, $LC_{90,}$ and mortality data were calculated using SPSS software package version 22.0 (SPSS Inc., Chicago, IL, USA). The antioxidant (ABTS) and percentage of hemolysis were calculated using MS Excel and relevant graphs were prepared using Prism 5 software. All tests were performed in triplicate and their data has been presented as mean ± SD.

Results

Biophysical Characterizations

UV-visible spectrophotometric data were recorded to study the effect of reaction time and pH in the synthesis of ZnO-APNPs. The color of the reaction mixture changed from green to light brown with the formation of a precipitate that confirmed the formation of nanoparticles. Greenish-black colored nanoparticles were obtained after overnight drying the pellet (Fig. 1).

FTIR spectrum of *A. paniculata* extract and ZnO-APNPs is shown in (Fig. 2). The major peaks of the IR spectra along with their wave number and possible functional groups have been appended in (Table 1). The FTIR spectrum of *A. paniculata* extract was used to identify the functional groups of different

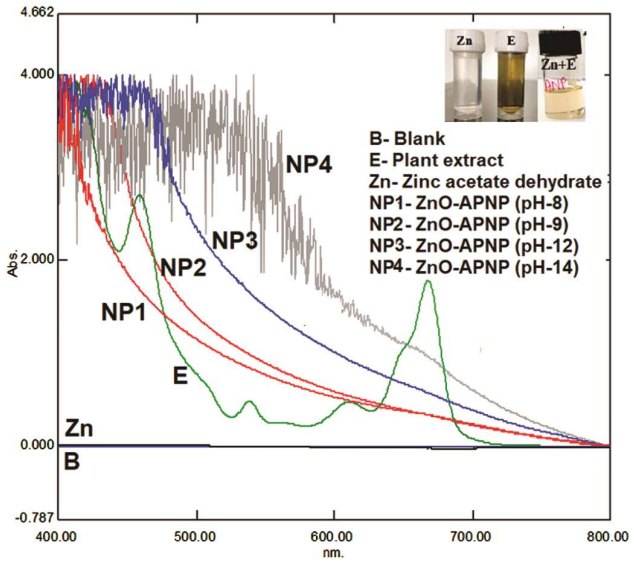

Fig. 1 — UV–Visible absorption spectra at different time intervals with anincreasing pH of *A. paniculata* nanoparticles (AP-ZnONPs). Blank (Dark Blue); Plant extract (Green); Zn acetate dehydrate (Black); NP1 (Red); NP2 (Pink); NP3 (Light Blue); NP4 (Grey)

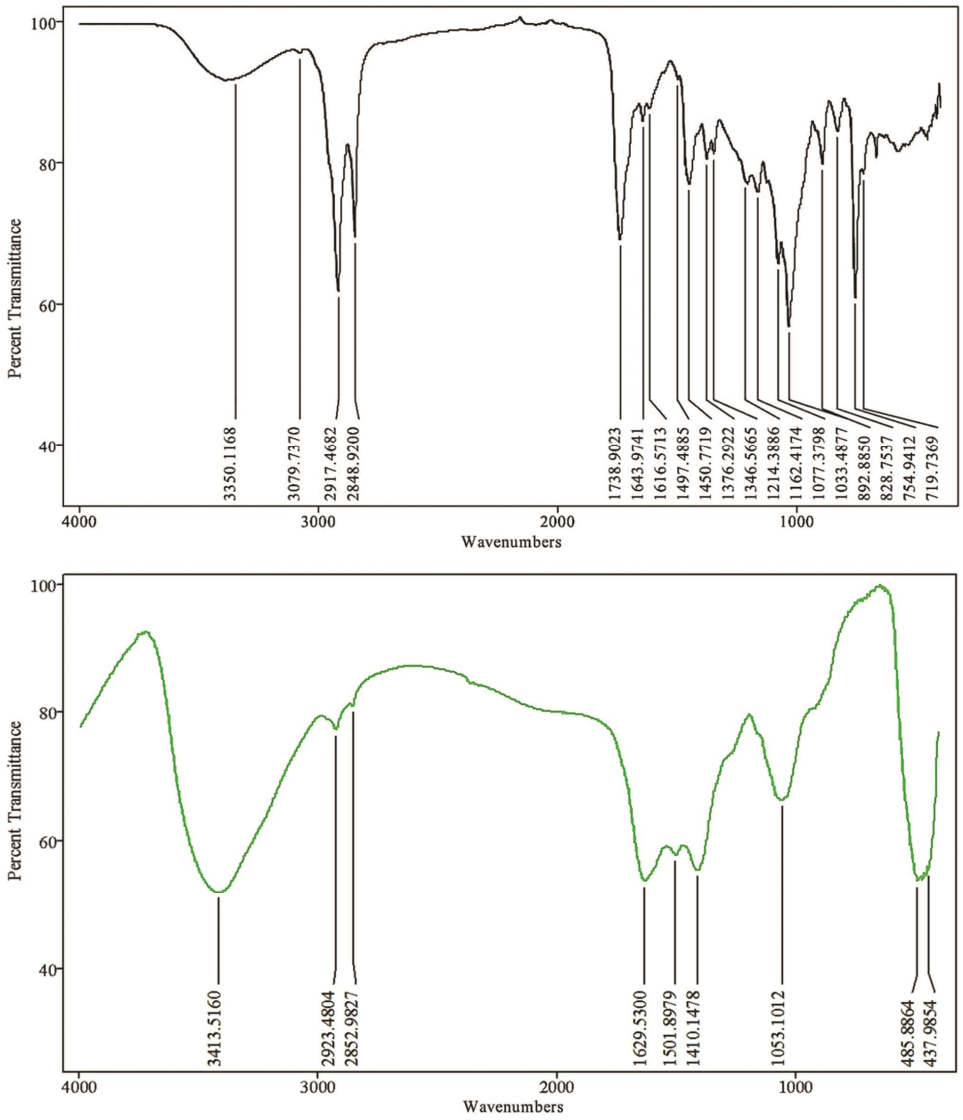

Fig. 2 — FTIR spectrum was measured in the range 4000–400 cm^{-1}. (A) Green synthesized ZnONPs using *A. Paniculata* (AP-ZnONPs); and (B) *A. paniculata* aqueous extract

components based on the peak value in the region of infrared radiation.

XRD is a well-established technique for the measurement of size, shape, and crystal structures of inorganic, organic, or metal-based nanomaterials[25]. It offers high spatial resolution at the atomic scale but it is limited to crystalline materials and has a lower intensity compared to electron diffraction. XRD profile for *A. paniculata* was obtained for analyzing chemical structure, elemental composition, and stereochemistry of ZnO-APNPs for confirming the crystal structure as shown in (Fig. 3). The obtained peaks corresponding with those of hexagonal phase ZnO-APNPs were found at the lattice planes (100), (002) (101) (102) (110) (103), and (112) in the value 31.72°, 35.31°, 36.67°, 47.47°, 57.32°, 63.40°, and 69.36°, respectively. The average crystalline size of the green synthesized ZnO-APNPs was calculated using the Debye-Scherrer's equation ($D = K\lambda/b \cos\theta$), where K = 0.9, D = crystal size (Å), λ = X-ray wavelength, and β = corrected half-width of the diffraction peak. The maximum crystalline intensity (101) was observed at 17.3 nm, thus the crystal structure of ZnO-APNPs is found to be hexagonal crystalline in nature.

The analysis of the morphology and microstructure of the nanoparticles was done using TEM. It was also used for size measurement and size distribution[26].

Table 1 — FTIR spectrum of the biosynthesized ZnO nanoparticles ZnO-APNPs and *Andrographis paniculata* extracts

Andrographis paniculata extracts				ZnO-APNPs			
Wavenumber (Cm^{-1})	Probable functional group	Class/Bond	Intensity	Wavenumber (Cm^{-1})	Probable functional group	Class/Bond	Intensity
3436.0894	-OH- broad	Hydroxyl	Medium	3413.5160	-OH- broad	Hydroxyl	Strong
3079.7370	-C-H- stretch	Aromatic	Strong	2923.4804	-CH3-	Alkanes	Weak
2917.4682	-CH- stretch	Alkanes	Strong	2852.9827	-CH2-	Alkanes	Weak
2848.9200	-CH2-	Alkanes	Medium	1629.5300	-CH=CHR-	Aromatic	Strong
1738.9023	-C=O- stretch	Esters	Strong	1501.8979	-N=O-	Nitroso	Weak
1643.9741	-C=C- stretch	Alkanes	Weak	1410.1478	-C-C-	Aromatic	Medium
1616.5713	-C=C- stretch	Alkanes	Weak	1053.1012	-C=O- stretch	Alcohol	Strong
1497.4885	-C-C- stretch	Aromatic	Weak	485.8864	-C-H-wag	Alkyl halides	Strong
1450.7719	-CH2 and CH3-	Alkanes	Medium				
1376.2922	C-H bend	Alkanes	Weak				
1346.5665	-N-O	Aromatic Nitro	Weak				
1214.3886	-C-N- stretch	Amines	Weak				
1162.4174	-P-H- bending	Phosphine	Weak				
1077.3798	-C-O- stretch	Ethers	Weak				
1033.4677	C-N- stretch	Amines	Medium				
892.8850	=C-H-out of plane	Alkanes	Medium				
828.7537	-C-H-out of plane	Aromatic	Medium				
754.9412	-S-OR-	Esters	Strong				
719.7369	-C-H-out of plane	Aromatic	Weak				

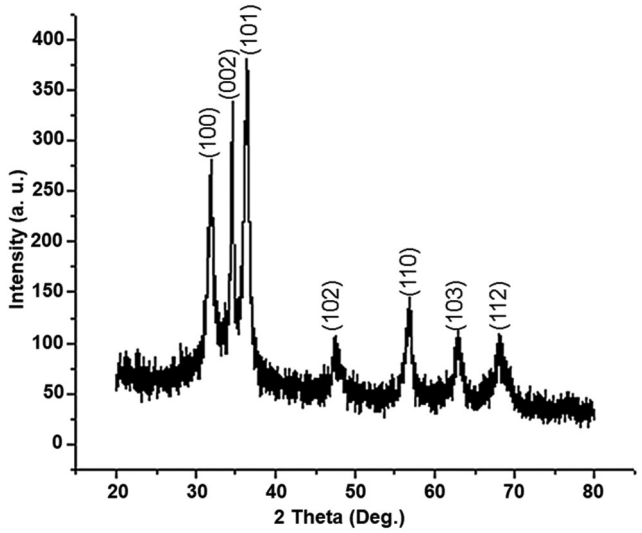

Fig. 3 — XRD pattern of green synthesized ZnONPs of *A. paniculata* (AP-ZnONPs).XRD was performed at parameters2Θ range of 20°-100°, at1.5406 A° wavelength

Figure 4 displays the scatter pattern or electron diffraction pattern of ZnO-APNPs indicating a polycrystalline structure. Figure 4 display the TEM images of ZnO-APNPs scanned at 500 nm that reveals that most of the ZnO-APNPs are quasi-spherical and their diameter is within the ~17 nm range.

Zeta potential is an important parameter of the characterization of nanoparticles that reflects the behavior of colloids. For stability, the shelf life of nanoparticles after the presence of surface charge in an electric field influencing nanoparticle movement, particles suspended in colloidal solution gave a mean potential of −10.4mV (Fig. 5). A mechanism for the synthesis of ZnO-NPs has been proposed in (Fig. 6).

ABTS antioxidant activity

ABTS is a radical scavenging assay that is used to evaluate the antioxidant activity of specific compounds. In the current study, concentration-dependent ABTS radical inhibition by ZnO-APNPs was found with a maximum inhibition of 39.51±1.25 at 100 mg/mL (Fig. 7). The results depicted that the green synthesized ZnO-APNPs exhibit significant free radical scavenging activity[27].

H_2O_2 activity

Hydrogen peroxide (H_2O_2) has strong oxidant capabilities that can kill microorganisms, plays a major role in cellular metabolism[28-29] and therefore used for medicinal purposes. It has an essential role in homeostatic metabolism, which is the major molecule in the third principle of the Redox Code of living organisms. The biological systems can produce hydrogen peroxide although hydrogen peroxide itself is not active, nonetheless, it can occasionally be toxic to cells, as it can give rise to hydroxyl radicals inside the cell[30]. H_2O_2 can also attack several cellular energy-producing systems. Figure 8 displays variations in the optical characteristics of ZnO-based

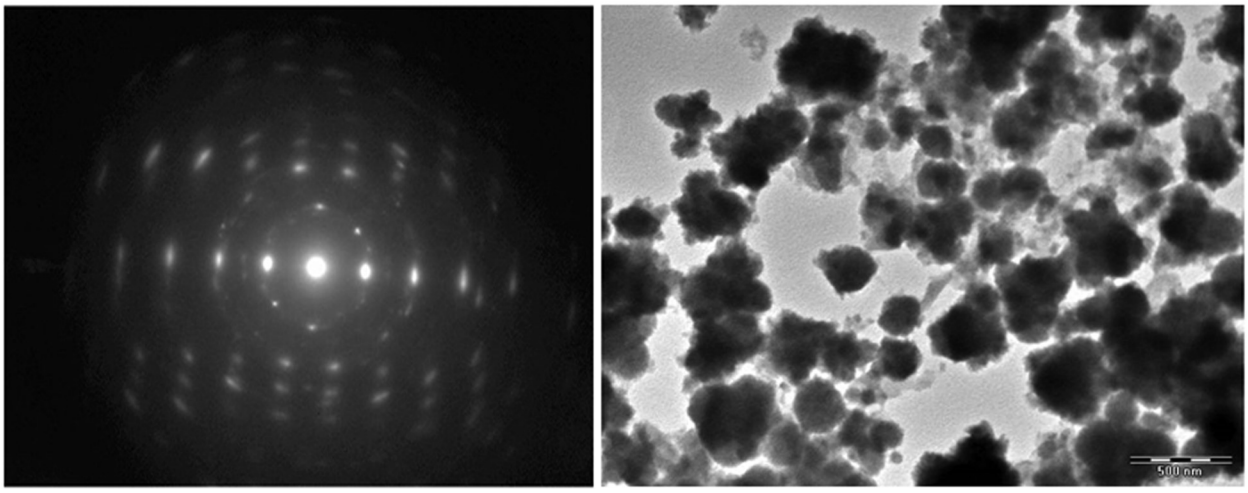

Fig. 4 — TEM image of green synthesized ZnONPs.(A) Electron diffraction pattern; and (B) TEM image showing the morphology of ZnONPs (magnification of 20,00,000X with ultra-high-resolution 0.2 nm)

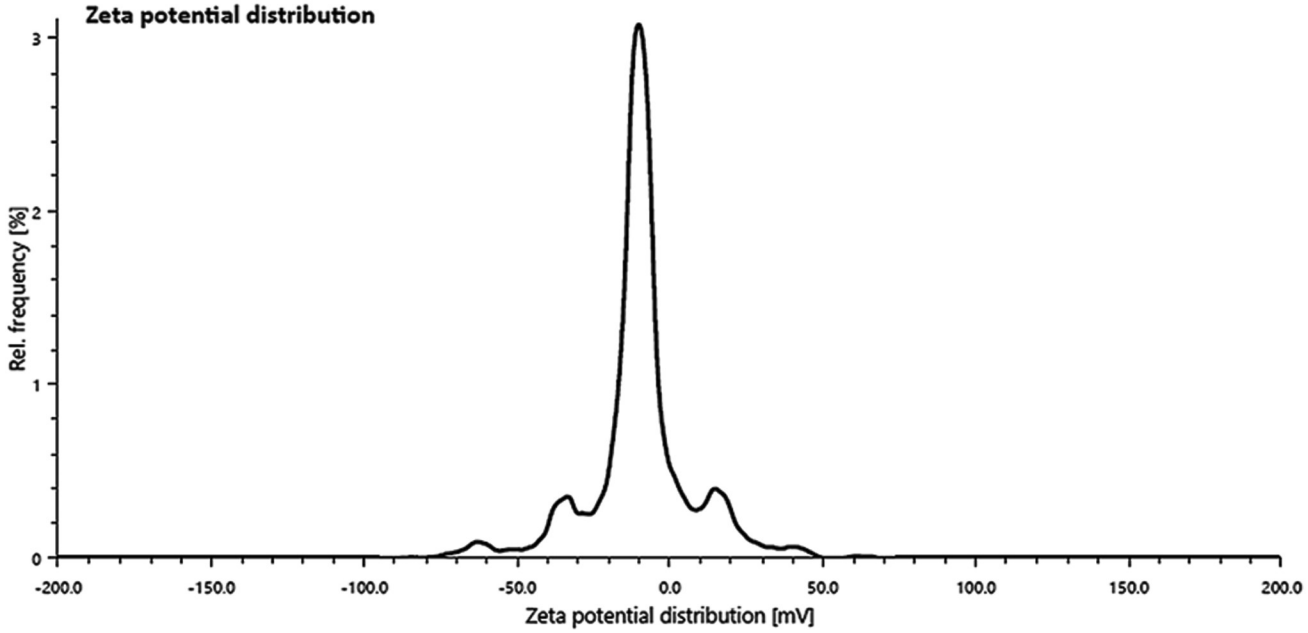

Fig. 5 — Zeta potential measurement pattern of *A. paniculata* (AP-ZnONPs). The measurements were analyzed with 1.5 Henry factor and 658 nm laser wavelength

nanoparticles with the time due to the addition of 20 mM H_2O_2.ZnO-APNPs displayed a decrease in absorbance with the increase in reaction time.

Larvicidal activity

Table 2 displays the percentage mortality of larvae at various concentrations tested and calculated LC_{50} and LC_{90} values after 24 h and 48 h of exposure. The larvicidal activity of the prepared ZnO-APNPs was tested for various concentrations 10, 50, 100, 200, 300, and 500 ppm against *A. culicifacies* larvae. Results displayed mortality percentages 11.56±0.11% (200 ppm), 19.47±1.10% (300 ppm), and 28.76±2.40% (500 ppm) after 24 h of exposure. The LC_{50} and LC_{90} values were 31.75±2.23 ppm and 189.56±2.44 ppm, respectively, at 24 h of exposure. The larvicidal activity was also tested for 48 h of exposure at the same concentrations mentioned above and the obtained mortality percentages were 24.16±0.22% (10 ppm), 38.74±1.15% (50 ppm), 55.61±1.55% (100 ppm), 69.16±1.01% (200 ppm), 84.47±1.35% (300 ppm) and 91.77±2.57% (500 pm). The LC_{50} and LC_{90} values were 95.45±1.56 ppm and 432.36±1.34 ppm, respectively, at 48 h of exposure (Table 2).

Morphological study

The microscopic image of the untreated larvae is displayed in (Fig. 9A). In the case of treated larvae, we can observe that the ZnO-APNPs penetrated deep into the body of the larvae due to the small size of the nanoparticles, while such observations were found to be missing for the untreated larvae. The microscopic image of the dead larvae clearly shows the deposition of nanoparticles on the surface of the mosquito body. Figure 9B & C displays ZnO-APNPs deposition on the larval body surface, head, and damaged thorax of the larvae whereas no such type of deposition can be seen in the body of untreated larva. The damage caused by zinc oxide nanoparticles in the eye, seta, and antenna is visible in (Fig. 9C), while palmate tufts/hairs (Fig. 9D) are also visible.

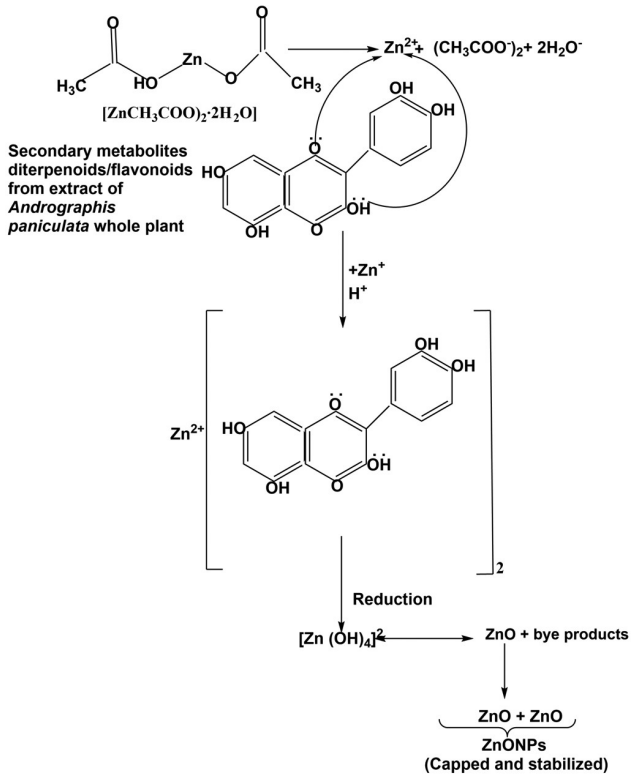

Fig. 6 — Proposed mechanism of synthesis of ZnONPs through *A. paniculata*

Toxicology assessment of ZnO-APNPs by *In vitro* hemolysis assay

We assessed the toxicity levels of the green synthesized ZnO-APNPs against human erythrocytes belonging to the 'A^+' positive blood group. As shown in (Fig. 10) the highest percentage of lysis was 9.81 at 25 µg/mL while it decreased to 9.19 on increasing the concentration of ZnO-APNPs to 200 µg/mL, respectively.

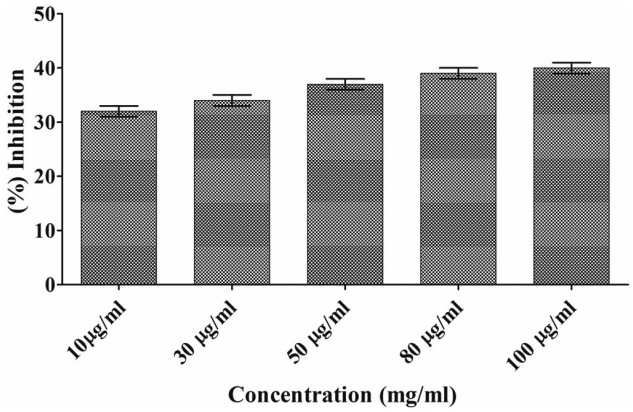

Fig. 7 — ABTS free radical scavenging assay of *A. paniculata* (AP-ZnONPs)

Table 2 — Results of Larvicidal activity (24 h and 48 h) of medicinal plant-based ZnO-APNPs tested against *Anopheles culicifacies*

Species	Concentration (ppm)	DMSO	Zinc acetate dihydrate	STD	AP-ZnONPs	Mortality (%)	LC_{50} (ppm)	LC_{90} (ppm)
Anopheles culicifacies					After 24 h			
	10	Nil	Nil	Temiphose	Nil	Nil	Nil	Nil
	50	Nil	Nil	Temiphose	Nil			
	100	Nil	Nil	Temiphose	Nil			
	200	Nil	Nil	Temiphose	Active	11.56±0.11	31.75±2.23	189.56±2.44
	300	Nil	Nil	Temiphose	Active	19.47±1.10		
	500	Nil	Nil	Temiphose	Active	28.76±2.40		
					After 48 h			
	10	Nil	Nil	Temiphose	Partial Active	24.16±0.22	95.45±1.56	432.36±1.34
	50	Nil	Nil	Temiphose	Partial Active	38.74±1.15		
	100	Nil	Nil	Temiphose	Initial Active	55.61±1.55		
	200	Nil	Nil	Temiphose	Initial Active	69.16±1.01		
	300	Nil	Nil	Temiphose	Highly Active	84.47±1.35		
	500	Nil	Nil	Temiphose	Highly Active	91.77±2.57		

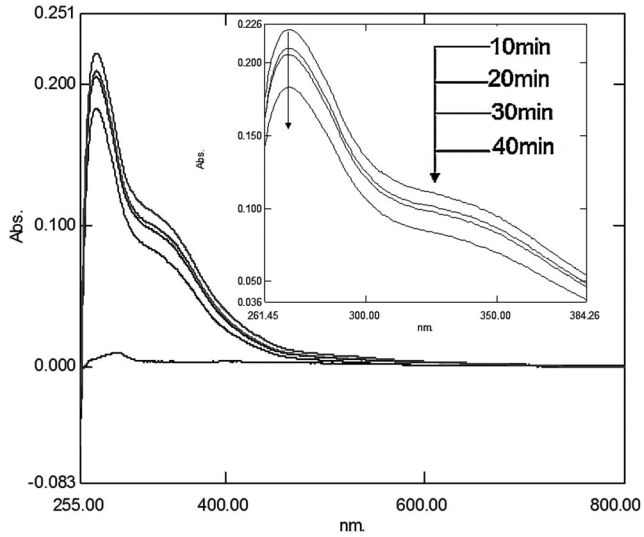

Fig. 8 — UV-visible absorbance spectra of *A. paniculata* (AP-ZnONPs) solution recorded at 10 min time intervals till 40 min after the addition of H_2O_2.

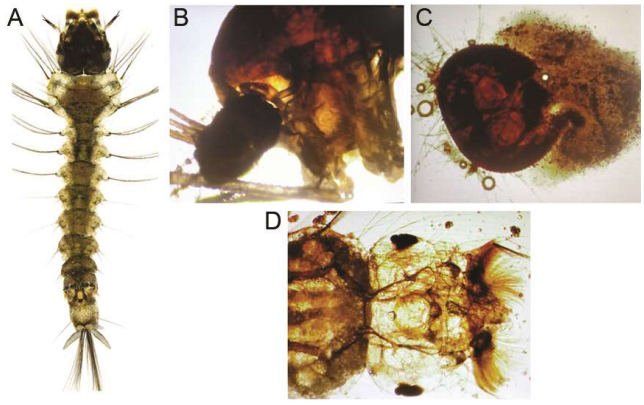

Fig. 9 — Larvicidal activity of *A. culicifacies* larvae (A) untreated larvae, (B) treated larvae showing damaged thorax, (C) head damaged, (D) Inner tufts/ hair/mouth damage at 100× magnification

DNA Binding

UV-vis spectral titration is one of the important tools for determining the DNA binding capacity of compounds. Prior to the addition of AP-ZnONPs, the stability of CT-DNA was examined at RT at 15 min intervals and was monitored for 1 h. The experiment was carried out keeping the concentration of AP-ZnONPs constant to which CT-DNA was gradually added. Successive binding of AP-ZnONPs with CT-DNA resulted in to decrease in absorption with significant, though minor, bathochromic effect or red-shift (240 nm to 320 nm) in the spectrum indicating that AP-ZnONPs preferably interact with DNA (Fig. 11). Absorption spectra of CT-DNA showed a hyperchromic effect with an isosbestic point, which indicates a very strong interaction between NPs and CT-DNA[24].

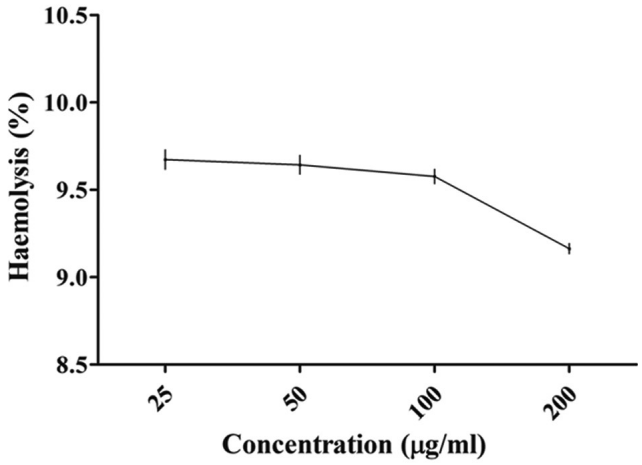

Fig. 10 — The percent hemolysis toxicity assay of larvicidal active *A. paniculata* (AP-ZnONPs) on human erythrocytes

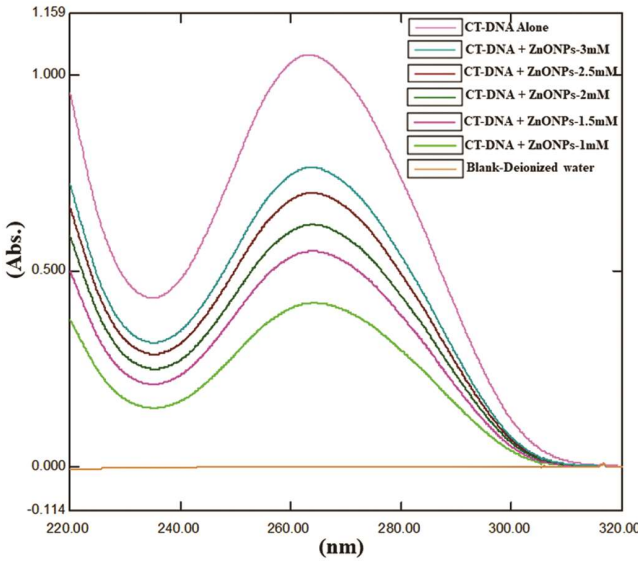

Fig.11 — UV-vis absorption spectra (220 nm to 320 nm) of *A. paniculata* (AP-ZnONPs) with CT-DNA at various concentrations of CT-DNA (1 mM–3 mM)

Discussion

Previously, we have reported on the *In vitro* antimalarial activity of *A. paniculata* extracts against the human malarial parasite *P. falciparum* and found promising results[31]. Further, the LC-MS analysis of the active extract led to the identification of 59 compounds that were mainly flavonoids and diterpenoids[31]. Owing to the presence of several compounds that might be responsible for the potential antimalarial activity and thus might have larvicidal properties, we selected *A. paniculata* for the green ZnO nanoparticle synthesis. *A. paniculata* whole plant extract was collected from healthy plants which

contain diterpenoids and flavanones as major constituents. During the Zinc oxide nanoparticles synthesis, the color of the assay mixture changed from green to yellow. The phytoconstituents of *A. paniculata* acted as a reducing and stabilizing agent for the formation of zinc oxide nanoparticles.

As compared to the sharp peak of the extract, we observed a peak obtained for ZnO-APNPs at 450 nm to 550 nm as we increased the pH from 9-14. The decline in sharpness of the peak might be due to the capping of Zinc oxide (ZnO-APNPs) by the metabolites present in the plant extract. Figure 1 demonstrates that the intensity of the peaks continued to increase at different time intervals with the same absorption maxima. The formation of ZnO nanoparticles has been reported earlier with absorption peaks at 330 nm, to 370 nm and 280 nm to 350 nm, at room temperature (RT) respectably[32]. Similar findings have been reported by Vimala *et al*. 2014, that the absorbance spectra of ZnO-NPs were recorded between 330 and 370 nm[33]. In our study, we performed at different time intervals in continuous heating with an increasing stirrer and recorded the UV-Visible spectrum in the same absorption maxima. Temperature and pH play important roles in nanoparticle formation. At RT above (28°C to 38°C) and at pH 12 the synthesized nanoparticles display peaks at near UV or visible region suggesting metal oxide reduction and synthesis[34]. The shape of the band was symmetrical, suggesting a uniform scattering of spherical shape nanoparticles. It has been reported that the absorption edge systematically shifts to the lower wavelength or higher energy with the decreasing size of the nanoparticle[35]. Therefore, UV-Visible spectrometry is the best technique for the detection of the formation, shape, and stability of nanoparticles in an aqueous solution.

Through FTIR analysis we were able to confirm the presence of Hydroxyl, Alkanes, Alkanes, Aromatic, Nitroso, Aromatic, Alcohol, and Alkyl halides compounds that are vital functional groups present in *A. paniculata* extract and in ZnO-APNPs. The hydroxyl group (–OH) indicates the presence of flavonoids, alcohol, alkaloids, and phenolic compounds. The presence of alkanes, and aromatic compounds confirm the presence of alkaloids in *A. paniculata* extract. Devasenan *et al*., 2016 reported the presence of primary and secondary amines, alcohols, aliphatic, aromatic amines, polysaccharides, alcohols, phenolic groups, nitro-compounds, and amides compounds in *A. paniculata* ZnO nanoparticles[36]. The results of the analysis clearly predict that the phytochemicals present in the *A. paniculata* extract might be responsible for the reduction, capping, prevented agglomeration, and stabilized ZnO-APNPs.

The crystal structure of ZnO-APNPs is found to be hexagonal crystalline in nature. Several studies have reported the hexagonal crystalline structure of ZnO nanoparticles. A pure hexagonal wurtzite structure for ZnO-NPs has also been reported using diffraction peaks (2θ degree) and attributed to the following Miller–Bravais indices: (100), (002), (101), (102), (110), (103), (200), (112), and (201) [46-48]. Bindu and Thomas analyzed the lattice strain in ZnO-NPs with crystalline sizes of 27.49 nm, 35.35 nm, 36.28 nm, 36.09 nm, and 34.55 nm[37]. Rajakumar *et al*., 2018 reported similar results and found a hexagonal zinc oxide phase, a well-crystalline particle structure[38]. The image clearly shows the presence of secondary material capping which may be assigned to bio-organic compounds present in the whole plant parts extract that confirm by observing sharp reflection in the XRD spectrum.

The particle size determined by the TEM analysis is in good agreement with that of the XRD analysis. The diameter of the spherical crystals of ZnO-NPs was reported to be between 13- 23 nm as analyzed using the HR-TEM[26]. In a previous studies using ZnO nanoparticles and TEM analysis, a size of 13.8nm was observed that was with the agreement of the XRD pattern[38].

A mean potential of −10.4mV was observed that suggested that the synthesized nanoparticles are negatively charged and moderately dispersed in the medium. The results support the stable synthesis of ZnO-APNPs that were stable in nature and with a shelf life of 2-3 months. We propose that the phytoconstituents that may reduce Zn^{2+} to ZnO, and further to ZnO nanoparticles aggregates are diterpenoids, and flavonoids that are present in high quantities in the *A. paniculata* extract[31] and may act as stabilizing and capping agents, respectively. The improved bioactivities of greens synthesized nanoparticles have been attributed to the plant-derived functional groups in these nanoparticles. The enhanced biosynthesis of diterpenoids and flavonoids has been related to the high capacity of compounds to chelate metals. Diterpenoids/flavonoids that possess

three potential bidentate binding sites, namely α-hydroxy-carbonyl, β-hydroxy-carbonyl, or catechol having two –OH groups in ortho positions, can form a stable complex with metal Zn cation. Therefore, the proposed theory of the formation of ZnO-APNPs involves the ionization of zinc acetate dehydrate in an aqueous medium to give Zn2+ which was reduced by principal phytochemicals present in the aqueous extract of *A. paniculata* extract to generate ZnO, which further aggregates to ZnO-NPs as shown in (Fig. 6).

Several chronic health problems resulting from free radicals can be minimized by preventing the formation of free radicals. Research is underway to find novel sources of antioxidants of natural origin that are economically viable and harmless. The green synthesized ZnO-APNPs exhibited significant free radical scavenging activity. A visible shift in the UV-Vis spectrum was obtained with increased reaction time leading to the conclusion that ZnO-APNPs were degraded when reacted with H_2O_2 along with the formation of free radicals (Fig. 8). ZnO-APNPs display that the antioxidant property may be due to the electron-donating property of the oxygen atoms in ZnO nanomaterial. The antioxidant behavior of the synthesized ZnO-APNPs makes them very useful for the treatment of several diseases caused due to oxidative stress.

The results of the larvicidal assays clearly demonstrated that ZnO-APNPs were able to induce mortality in *A. culicifacies* larvae and could be a potential larvicidal agent. The morphological results make it clear that the larval death might have occurred due to the morphological damage to the different organs of the larvae caused by the accumulation of ZnO-APNPs that might have reacted with the cellular proteins and thereby hinder the enzymatic reactions in the larvae. However, the precise mechanism by which mosquito larvae are killed by nanoparticles is not known and needs further comprehensive study. The particular mechanism of action involved in the larvicidal activity of ZnO-APNPs is still required to be fully unveiled. Green synthesized ZnO-APNPs may induce the generation of Reactive Oxygen Species and causes membrane dysfunction. For the reason that ZnO-APNPs can impair the enzymes/proteins involved in cell wall synthesis. Several reports have been published on the larvicidal activity of plant-based nanoparticles but the particular mechanism of action behind this phenomenon is not fully understood. Even few researchers have reported that the small size of Zinc oxide nanoparticles can easily penetrate the insect gut wall and bind to sulfur and phosphorus groups of deoxyribonucleic acid affecting its normal functioning and ultimately leading to cell death.

ZnO-APNPs toxicity was analyzed by performing the hemolytic assay. Investigations on the cytotoxicity of the ZnO-APNPs against human RBC may provide us with novel insights into the safety of nanoparticles. The blood cells (particularly erythrocytes) being major players of the circulatory system are the major cells that can be affected by nanoparticles that might affect the cardiovascular system and thus other organs causing considerable damage such as cell membrane injury. The biodegradation of zinc oxide nanoparticles and their effect on erythrocytes is of prime importance. The results proved that ZnO-APNPs mediated synthesized zinc oxide nanoparticles are not only safer for human use but the hemolysis also decreased on increasing the concentration of the nanoparticles. The ZnO-APNPs can find multiple uses in biomedical applications and for various pharmacological purposes. In the current study, we successfully synthesized and performed larvicidal activity and antioxidant ZnO-APNPs with the aqueous method. The effective larvicidal potential of ZnO nanoparticles with antioxidant properties may allow them to be used in healthcare products and more importantly nanomedicine preparations.

The DNA binding studies indicated that the ZnO-APNPs might be interacting with the larval DNA and might be interfering with some genes that codes for major metabolic enzymes or proteins required for the survival of the larvae. Interaction of gold nanoparticles (AuNPs) with *E. coli* DNA leading to DNA damage has earlier been reported[39]. The absorption spectra of CT-DNA showed a hyperchromic effect with an isosbestic point, which indicates a very strong interaction between NPs and CT-DNA.

Conclusion

Nanoparticles have become a vital tool for research in the current period due to their wide application in very nearly every field, especially in medical science. In conclusion, synthesized Zinc oxide nanoparticles through the green synthesis method which is pollution-free and eco-friendly. The ZnO-APNPs were characterized using UV–Vis spectra, FTIR, and

TEM analysis. TEM revealed the morphology of the synthesized nanoparticles to be crystalline with a size range of 17 nm. The results displayed the formation of ZnO-APNPs with illustrious hexagonal morphology. XRD results also supported the analysis of crystalline nature and particle size in the nano range. The ZnO-APNPs were formed due to the influence of phytochemicals or secondary metabolites such as Hydroxyl, Alkanes, Alkanes, Aromatic, Nitroso, Aromatic, Alcohol, and Alkyl halides groups that have interacted with the zinc surface. ZnO-APNPs exhibited potent larvicidal activity against *A. culicifacies* larvae having mortality percentages of 91.77±2.57% at 500 pm after 48 h of exposure. The LC_{50} and LC_{90} values were 95.45±1.56 ppm and 432.36±1.34 ppm respectively at 48h of exposure. The DNA binding assay displays molecular interactions between the ZnO-APNPs and the DNA. The binding of ZnO-APNPs can lead to structural and functional modification of larval DNA and thus might impair major metabolic pathways leading to larval death. The exact mechanism of ZnO-APNPs activity is required to be deciphered. There were no signs of toxicity to human RBCs as observed in the hemolytic assay. The ZnO-APNPs also displayed significant antioxidant activities observed by 39.51% inhibition of ABTS free radical. Biosynthesized ZnO-APNPs prepared from *A. paniculata* are expected to have notable applications in pharmaceutical and biomedical fields such as drug delivery and cosmetics such as mosquito creams/lotion. Hence, overall, the biocompatibility of these zinc oxide nanoparticles is to be considered nontoxic, and in these coming circumstances, it can be used for pest management and drug delivery to the human affected by infectious pathogens.

Acknowledgement

The Authors would like to thank UGC-DAE Consortium for Scientific Research, Indore, Madhya Pradesh, India for FTIR, XRD, and TEM analysis.

Conflict of interests

All authors declare no conflict of interest.

References

1 Suresh M, Jaison J, Chan YS, Danquah MK & Kalaiarasi JMV, Opportunities for Metal Oxide Nanoparticles as a Potential Mosquitocide. *BioNano Sci,* 10 (2019) 292.

2 Harbach RE, The Culicidae (Diptera): A Review of Taxonomy, Classification, and Phylogeny. *Zootaxa,* 1668 (2007) 591.

3 Benelli G, Plant-Borne Ovicides in the Fight against Mosquito Vectors of Medical and Veterinary Importance: A Systematic Review. *Parasitol Res,* 114 (2015) 3201.

4 Heinz M, Arthropods as Vectors of Emerging Diseases. *Parasitology Research Monographs, Springer*: Heidelberg, New York, 388 (2012).

5 Rueda LM, Global Diversity of Mosquitoes (Insecta: Diptera: Culicidae) in Freshwater. *Hydrobiologia,* 595 (2008) 477.

6 Amutha V, Arul D, Santhanam P, Ballamurugan AM & Perumal P, Mosquito-Larvicidal Potential of Metal and Oxide Nanoparticles Synthesized from Aqueous Extract of the Seagrass *Cymodocea Serrulate*. *J Clust Sci,* 30 (2019) 797.

7 WHO, Malaria (Malaria report, 2021, WHO); (2021)Available from: https://www.who.int/news-room/fact-sheets/detail/mala ria

8 Govindarajan R, Vijayakumar M & Pushpangadan P, Antioxidant approach to disease management and the role of 'Rasayana' herbs of Ayurveda. *J Ethnopharmacol*, 99 (2005) 65.

9 Singha PK, Roy S & Dey S, Antimicrobial activity of *Andrographis paniculata*. *Fitoterapia*, 74 (2003) 692.

10 ChaoWW, Isolation and identification of bioactive compounds in *Andrographis paniculata* (Chuanxinlian). *Chinese Medi*, 5 (2010) 17.

11 Jarukamjorn K & Nemoto N, Pharmacological aspects of *Andrographis paniculata* on health and its major diterpenoid constituent and rographolide. *J Health Sci,* 54 (2008) 370.

12 Ramesh P, Rajendran A & Meenakshi sundaram M, Green synthesis of zinc oxide nanoparticles using flower extract *Cassia auriculata*. *J Nanosci Nanotechnol,* 1 (2014) 41.

13 Sukumar K, Perich MJ & Boobar LR, Botanical derivatives in mosquito control: a review. *J Am Mosq Control Assoc*, 7 (1991) 210.

14 Giovanni B, Alice C & Angelo C, Nanoparticles for mosquito control: Challenges and constraints. *J King Saud Univ Sci,* 29 (2017) 424.

15 Rouhi J, Mahmud S, Naderi N, Ooi CR & Mahmood MR, Physical properties of fish gelatin-based bio-nanocomposite films incorporated with ZnO nanorods. *Nanoscale Res Lett,* 8 (2013) 364.

16 Baby VS & Sriman NJ, Characterization studies on medicinal plant of *Andrographis paniculata* (NEES). *JMPS*, 3 (2015) 96.

17 Sareer O, Ahad A & Umar S, Prophylactic and lenitive effects of Andrographis paniculata against common human ailments: an exhaustive and comprehensive reappraisal. *J Pharm Res Opin,* 2 (2012) 138.

18 Sajeeb BK, Kumar U, Halder S & Sitesh CB, Identification and Quantification of Andrographolide from *Andrographis paniculata* (Burm. f.) Wall. ex Nees by RP-HPLC Method and Standardization of its Market Preparations. *J Pharm Sci,* 14 (2015) 71.

19 Konduri VV , Kalagatur NK, Nagaraj A, Kalagadda VR, Mangamuri UK, Durthi CP & Poda S, *Hibiscus tiliaceus* mediated phytochemical reduction of zinc oxide nanoparticles and demonstration of their antibacterial, anticancer, and dye degradation capabilities. *Indian J Biochem Biophys,* 59 (2022) 565.

20 Singh K, Chopra DS, Singh D & Singh N, Green synthesis and characterization of iron oxide nanoparticles using

Coriandrum sativum L. leaf extract. *Indian J Biochem Biophys,* 59 (2022) 450.

21 Dinesh R, Anandaraj M, Kumar A, Bini YK, Subila KP & Aravind R, Isolation, characterization, and evaluation of multi-trait plant growth promoting rhizobacteria for their growth promoting and disease suppressing effects on ginger. *Microbiol Res*, 173 (2015) 34.

22 Finney DJ, Probit Analysis. *Cambridge University Press*: London, (1971) 68.

23 Sanaeimehr Z, Javadi I and Namvar F, Antiangiogenic and antiapoptotic effects of green-synthesized zinc oxide nanoparticles using *Sargassum muticum* algae extraction. *Cancer Nanotechnol*, 9 (2018) 3.

24 Singh A, Neelama & Mahima K, Physicochemical investigations of zinc oxide nanoparticles synthesized from *Azadirachta Indica* (Neem) leaf extract and their interaction with Calf-Thymus DNA. *Results Phys,* 13 (2019) 102168.

25 Marslin G, Siram K, Maqbool Q, Selvakesavan R, Kruszka D, Kachlicki P & Franklin G, Secondary Metabolites in theGreen Synthesis of Metallic Nanoparticles. *Materials Basel,* 11 (2018) 940.

26 Rasmussen K, Rauscher H, Mech A, RiegoSintes J, Gilliland D & González M, Physico-chemical properties of manufactured nanomaterials-Characterisation and relevant methods. An outlook based on the OECD Testing Programme. *Regul Toxicol Pharmacol,* 92 (2018) 8.

27 Siddiqi KS, Rahman AU, Tajuddin HA, Properties of Zinc Oxide nanoparticles and their activity against microbes. *Nanoscale Res Lett,* 13 (2018) 141.

28 Corpuz AV & Marlou RS, Larvicidal Activity of Papaya (*Carica Papaya*) and Madre de Cacao (GliricidiaSepium) leaf extracts against *Aedes aegypti*. *Int J Sci Eng Res,* 10(2019) 1163.

29 Chandrasekaran R, Seetharaman P, Krishnan M, Gnanasekar S & Sivaperumal S, *Carica Papaya* (Papaya) Latex: A new paradigm to combat against dengue and filariasis vectors *Aedes aegypti* and *Culex quinquefasciatus* (Diptera: Culicidae). *3 Biotech,* 8 (2018) 83.

30 Jinhuan J, Jiang P & Jiye C, The advancing of Zinc Oxide nanoparticles for biomedical applications. *Bioinorg Chem Appl,* (2018) 1062562.

31 Dwivedi MK, Mishra S, Sonter S & Singh PK, Diterpenoids as potential anti-malarial compounds from *Andrographis paniculata*. *Beni Suef Univ J Basic Appl Sci,* 10 (2021) 7.

32 Kavitha S, Dhamodaran M & Prasad R, Synthesis and characterization of zinc oxide nanoparticles using terpenoid fractions of *Andrographis paniculata* leaves. *Int Nano Lett,* 7 (2017) 141.

33 Vimala K, Sundarraj S & Paulpandi M, Green synthesized doxorubicin loaded zinc oxide nanoparticles regulates the Bax and Bcl-2 expression in breast and colon carcinoma. *Process Biochem,* 49 (2014)160.

34 Gupta M, Tomar RS, Kaushik S, Mishra RK & Sharma D, Effective Antimicrobial Activity of Green ZnO Nano Particles of Catharanthus roseus. *FrontMicrobiol*, 9 (2018) 2030.

35 Gupta A, Srivastava P, Bahadur L, Amalnerkar DP & Chauhan R, Comparison of physical and electrochemical properties of ZnO prepared via different surfactant-assisted precipitation routes. Appl Nanosci, 5 (2015) 787.

36 Devasenan S, Beevi NH & Jayanthi SS, Green Synthesis and Characterization of Zinc Nanoparticle Using *Andrographis paniculata* Leaf Extract. *Int J Pharm Sci Rev Res*, 39 (2016) 243.

37 Bindu P & Thomas S, Estimation of Lattice Strain in ZnO Nanoparticles: X-Ray Peak Profile Analysis. *J Theor Appl Phys,* 8 (2014) 123.

38 Rajakumar G, Thiruvengadam M, Mydhili G & Gomathi T, Green approach for synthesis of zinc oxide nanoparticles from *Andrographis paniculata* leaf extract and evaluation of their antioxidant, anti-diabetic, and anti-inflammatory activities. *Bioprocess Biosyst Eng,* 41 (2018) 21.

39 Setia VY, Dangi K, Biswas L, Singh P & Verma AK, Nano-therapeutic efficacy of green synthesized gold nanoparticles (gAuNPs) and its antibacterial efficacy. *Indian J Biochem Biophys.* 59 (2022) 455.